Teal: Learning-Accelerated Optimization of WAN Traffic Engineering

Zhiying Xu
Harvard University

Francis Y. Yan
Microsoft Research

Rachee Singh
Cornell University

Justin T. Chiu
Cornell University

Alexander M. Rush
Cornell University

Minlan Yu
Harvard University

ABSTRACT

The rapid expansion of global cloud wide-area networks (WANs) has posed a challenge for commercial optimization engines to efficiently solve network traffic engineering (TE) problems at scale. Existing acceleration strategies decompose TE optimization into concurrent subproblems but realize limited parallelism due to an inherent tradeoff between run time and allocation performance.

We present Teal, a learning-based TE algorithm that leverages the parallel processing power of GPUs to accelerate TE control. First, Teal designs a flow-centric graph neural network (GNN) to capture WAN connectivity and network flows, learning flow features as inputs to downstream allocation. Second, to reduce the problem scale and make learning tractable, Teal employs a multi-agent reinforcement learning (RL) algorithm to independently allocate each traffic demand while optimizing a central TE objective. Finally, Teal fine-tunes allocations with ADMM (Alternating Direction Method of Multipliers), a highly parallelizable optimization algorithm for reducing constraint violations such as overutilized links.

We evaluate Teal using traffic matrices from Microsoft's WAN. On a large WAN topology with >1,700 nodes, Teal generates near-optimal flow allocations while running several orders of magnitude faster than the production optimization engine. Compared with other TE acceleration schemes, Teal satisfies 6–32% more traffic demand and yields 197–625× speedups.

CCS CONCEPTS

• **Networks → Traffic engineering algorithms**; • **Computing methodologies → Machine learning**.

KEYWORDS

Traffic Engineering, Wide-Area Networks, Network Optimization, Machine Learning

1 INTRODUCTION

Large cloud providers invest billions of dollars to provision and operate planet-scale wide-area networks (WANs) that interconnect geo-distributed cloud datacenters. Cloud WANs play a vital role in the operations of cloud providers as they enable low-latency and high-throughput applications in the cloud. Over the last decade, cloud providers have implemented centralized network traffic engineering (TE) systems based on SDN (software-defined networking) to efficiently utilize their cloud WANs [21, 22, 25, 33].

TE systems allocate demands between datacenters to achieve high link utilization [21, 25], fairness among network flows [21], and resilience to link failures in WANs [4, 38]. Traditionally, cloud WAN TE systems have approached traffic allocation as an optimization problem, with the objective of achieving a desired network property (e.g., minimum latency, maximum throughput). To this end, they implement a software-defined TE controller as illustrated in Figure 1. The TE controller periodically (e.g., every five minutes) receives traffic demands to allocate gauged by a bandwidth broker, solves the TE optimization problem, and translates the traffic allocations into router configurations to deploy through SDN.

After a decade of operation, production WAN TE systems are facing two major challenges. First, the deployment of new edge sites and datacenters has increased the size of cloud WANs by an order of magnitude [21]. Larger WAN topologies have increased the complexity of TE optimization and the time required to solve it. During the computation of updated flow allocations (even when the five-minute time budget is not exceeded), stale routes will remain in use and lead to suboptimal network performance [2]. Second, WANs have evolved from carrying first-party discretionary traffic to real-time and user-facing traffic [34]. As a result, cloud TE systems must react to rapid changes in traffic volume, which is a hallmark of organic user-driven demands. Sudden topology changes due to link failures further exacerbate the negative effects of long TE control on network performance. Therefore, fast computation of traffic allocations is critical for TE systems to retain performance on large WAN topologies.

While linear programming (LP) solvers used by TE systems can find optimal solutions, they struggle to scale with the growing network size. State-of-the-art algorithms designed for accelerating TE optimization address this challenge by decomposing the original problem into smaller subproblems (through the partition of WAN topology [2] or traffic demands [46]), and solve them in parallel using LP solvers. However, these algorithms face a fundamental tradeoff between speed and performance in the decomposition, restricting themselves to only *a few dozen* subproblems and thus limited parallelism (§2.1).

Our key insight is that deep learning-based TE schemes may unlock massive parallelism by utilizing *thousands of* GPU threads that are made readily accessible through modern deep learning frameworks [7, 48, 56]. The enormous parallelism is owing to the well-known affinity between neural networks and GPUs (e.g., SIMD operations on GPUs speed up matrix multiplication), as well as the tremendous community efforts for optimizing neural network inference [24, 27, 57]. Meanwhile, by capitalizing on a wealth of historical data from production WANs and exploiting traffic patterns,

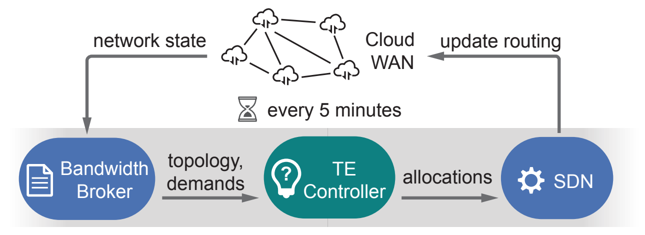

Figure 1: Control loop of WAN traffic engineering.

learning-based algorithms are poised to simultaneously retain TE performance as well.

Unfortunately, off-the-shelf deep learning models do not directly apply to TE. First, standard fully-connected neural networks fail to take into account the effects of WAN connectivity on traffic allocations, yielding solutions that are far from optimal. Second, the escalating scale of the TE problem makes it intractable to train a monolithic model to navigate the high-dimensional solution space. Finally, neural networks are unable to enforce constraints, leading to unnecessary traffic drops due to exceeded link capacities.

To address these challenges, we present a learning-accelerated TE scheme named Teal. First, Teal constructs a flow-centric graph neural network (GNN) to capture WAN topology and extract informative features from traffic flows for the downstream allocation task. Next, Teal allocates each demand individually using a shared policy (neural) network based on the learned features. Doing so reduces the problem scale from global traffic allocation to per-demand tasks, making the learning process more tractable (in a low-dimensional space) and feasible (fit into GPU memory). To coordinate the independent allocations of demands and avoid contention for links, Teal leverages multi-agent reinforcement learning (RL) to train the end-to-end model—GNN and policy network—toward optimizing a central TE objective. Finally, Teal fine-tunes the model's output allocations using a highly parallelizable constrained optimization algorithm—ADMM (alternating direction method of multipliers), which is well suited for reducing constraint violations such as oversubscribed links and enhancing solution quality.

We evaluate Teal on traffic matrices collected over a 20-day period from Microsoft's WAN (§5). Our experimental results show that on large WAN topologies, Teal realizes near-optimal flow allocation while being several orders of magnitude faster than the production TE optimization engine using LP solvers. Compared with the state-of-the-art schemes for TE acceleration [2, 45, 46] on a large topology with >1,700 nodes, Teal satisfies 6–32% more traffic demand and yields 197–625× speedups. To aid further research and development, we have released Teal's source code at https://github.com/harvard-cns/teal.

2 BACKGROUND AND MOTIVATION

Production WANs rely on a centralized TE controller to allocate traffic demands between datacenters, which are gauged by a bandwidth broker periodically (e.g., every 5 minutes). The TE controller splits the traffic demand onto a handful of precomputed paths (e.g., 4 shortest paths [2, 46]) between the demand's source and destination, with the goal of maximizing a TE objective (e.g., overall throughput) while satisfying a set of constraints (e.g., link capacities). This path formulation of TE is widely adopted in production inter-datacenter WANs [21, 22, 25, 33]. At its core, TE optimization is a multi-commodity flow problem (formally defined in Appendix A), which is traditionally solved with linear programming (LP) solvers. In this section, we begin with the scalability crisis faced by today's TE systems, and motivate the need and challenges for a learning-accelerated TE solution.

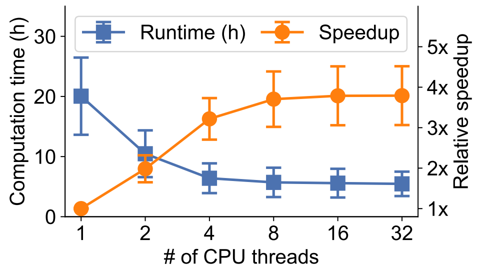

Figure 2: On a topology with >1,700 nodes (ASN in Table 1), the TE optimization using the Gurobi solver experiences a marginal speedup as more CPU threads become available.

2.1 Scaling challenges of TE

In their early years, cloud WANs only consisted of tens of datacenters, so it was feasible for commercial LP solvers to compute traffic allocations frequently. However, the rapid deployment of new datacenters has rendered the TE task prohibitively slow at scale, requiring hours for commercial solvers to allocate traffic on WANs with thousands of nodes. Consequently, WAN operators are seeking to accelerate TE optimization to keep pace with the growing size of the WAN.

Parallelizing LP solvers. An intuitive way of accelerating TE optimization is to parallelize state-of-the-art LP solvers, such as Gurobi [17] and CPLEX [23]. Figure 2 evaluates the speedup of the Gurobi solver on a WAN topology with more than 1,700 nodes (ASN in Table 1). As more CPU threads are made available, we observe that the speedup is sublinear and marginal. E.g., using 16 threads only makes Gurobi 3.8× faster, which still requires 5.5 hours to complete a flow allocation. This is due to LP solvers' sequential nature, e.g., the conventional simplex method [47] takes one small step at a time toward the optimal solution along the edges of the feasible region, and requires thousands to millions of such steps to complete. To exploit multiple CPU threads, LP solvers often resort to concurrently running *independent* instances of different optimization algorithms [1], where each instance executes serially on a separate thread; the solution is yielded by whichever instance completes first. This is apparently not an efficient use of CPU capacity, thus resulting in marginal speedups on multiple CPUs.

Approximation algorithms. Combinatorial algorithms, such as the Fleischer's algorithm [10], are designed to compute approximate but asymptotically faster solutions to the underlying network flow problem of TE. Despite having a lower time complexity than LP solvers in theory, these approximation algorithms are found to be hardly faster in practice [2]. The reason is that these algorithms remain *iterative* in nature, incrementally allocating more flows until the solution quality is deemed adequate (yet suboptimal), which often results in an excess of iterations to terminate.

Decomposing TE into subproblems. Recently, NCFlow [2] and POP [46] introduced techniques to decompose TE optimization into subproblems, applying LP solvers simultaneously in each subproblem and merging their results at the end. NCFlow partitions the network spatially into k clusters, whereas POP creates k replicas of the network, each with $1/k$ link capacities, and randomly assigns traffic demands to these replicas. Although a larger k reduces the overall run time, it also fundamentally impairs the TE performance. Moreover, NCFlow also requires nontrivial coordination during the merging process. Consequently, NCFlow and POP are forced to adopt small values of k (e.g., 64–81 on a network of 754 nodes). In §5, we show that NCFlow and POP are substantially slower than our learning-accelerated approach, while having notably worse allocation performance.

2.2 Accelerate TE optimization with ML

To cope with the growing scale of TE, we argue that with judicious design, machine learning (ML) can significantly accelerate TE optimization. By training on a vast amount of historical traffic data, ML-based TE schemes also have the potential to attain near-optimal allocation performance.

Unlocking massive parallelism. Encoding a TE algorithm in neural networks transforms the traditionally iterative TE optimization (LP solvers or combinatorial algorithms) into the inference process of neural networks, where the input data (e.g., traffic demands on a WAN topology) is propagated in the forward direction through the neural network to compute the output (e.g., traffic splits on the preconfigured paths). This inference process unlocks massive parallelism due to mainly consisting of highly parallelizable operations such as matrix multiplications.

Leveraging hardware acceleration. Modern deep learning frameworks [48, 56, 57] have empowered neural networks to easily leverage *thousands of* threads on GPUs (or other specialized hardware [16]). They can greatly accelerate the computation of learning-based TE systems compared with state-of-the-art schemes [2, 46], which are fundamentally limited to *tens of* parallel workers. In addition, the deep learning community has integrated various optimization techniques [24, 27, 57] into these frameworks, further accelerating neural network inference.

Exploiting abundant training data. Operational WANs generate an abundance of traffic data that can be used to train neural networks. A carefully designed ML-based TE scheme is capable of discovering regularities in the training data—such as patterns in graph connectivity, link capacities, and traffic demands—and ultimately learns to optimize allocation performance with respect to operator-specified objectives.

2.3 Challenges of applying ML to TE

While holding the promise of near-optimal performance and substantial speedup relative to LP-based TE methods, deep learning is not a panacea. In fact, using ML for TE optimization is not as straightforward as it may appear.

Graph connectivity and network flows. Naively using vanilla fully-connected neural networks for TE optimization would ignore the connectivity in WAN topology. While graph neural networks (GNNs) [50, 63], designed for graph-structured input data, can model traditional graph attributes such as nodes and edges, their unmodified form is inadequate to model network *flows*—the focal point of TE optimization.

High-dimensional solution space. In the path formulation of TE widely adopted in practice (details in Appendix A), the TE controller splits each demand across a handful of preconfigured paths, such as 4 shortest paths. Therefore, representing the flow allocation for a topology of N nodes requires $O(N^2)$ split ratios. To put it into context, on a topology with 1,000 nodes, the solution space would contain up to 4 million dimensions, exposing ML-based TE methods to the "curse of dimensionality" [32].

Constrained optimization. Unlike LP solvers, neural networks are known to lack the capability to enforce constraints on outputs [37]. As a result, the traffic allocations generated by neural networks may exceed certain link capacities when deployed directly, leading to network congestion and reduced TE performance.

To tackle the above challenges, we propose the following designs: *i)* a flow-centric GNN (called "FlowGNN") to capture WAN connectivity and model network flows (§3.2); *ii)* a multi-agent reinforcement learning (RL) algorithm that allocates each traffic demand independently to reduce the problem scale and make learning tractable (§3.3); *iii)* solution fine-tuning using the alternating direction method of multipliers (ADMM) to minimize constraint violations such as link overutilization (§3.4).

3 TEAL: LEARNING-ACCELERATED TE

In this section, we present the design of Teal—**T**raffic **E**ngineering **A**ccelerated with **L**earning. The goal of Teal is to train a fast and scalable TE scheme through deep learning while achieving near-optimal traffic allocation on large-scale topologies. The rationale behind using deep learning is to harness the massive parallelism and hardware acceleration unlocked by neural networks. Moreover, every component of Teal is carefully designed to be *parallelizable* (fast on GPUs) and *scalable* (performant on large WANs).

3.1 Overview

We begin by outlining the workflow of Teal during deployment (Figure 3). Upon the arrival of a new traffic demand matrix or a change in link capacity[1], Teal passes the updated traffic demands and current link capacities into a novel graph neural network (GNN) that we call *FlowGNN* (§3.2). FlowGNN learns to transform the demands into compact feature vectors known as "embeddings," which preserve the graph structure and encode the flow information required for the downstream allocation. These flow embeddings are extracted by FlowGNN in a parallel and parameter-efficient manner that scales well with the size of the WAN topology.

In the widely adopted path formulation of TE (details in Appendix A), each traffic demand is split into multiple flows over a set of preconfigured paths (e.g., 4 shortest paths [2, 46]). To determine the split ratios of a given demand, Teal aggregates the

[1]We note that link failures can be viewed as an extreme scenario of capacity change, where the capacity of a failed link is reduced to zero.

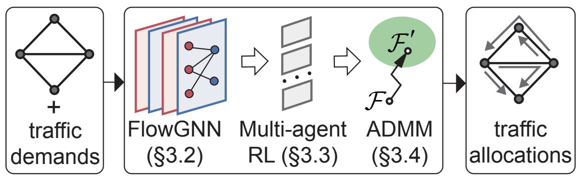

Figure 3: Workflow of Teal. Teal inputs traffic demands and link capacities into FlowGNN to learn flow embeddings (§3.2), which are then mapped to initial traffic allocations through multi-agent RL (§3.3). ADMM subsequently fine-tunes the allocations and mitigates constraint violations (§3.4).

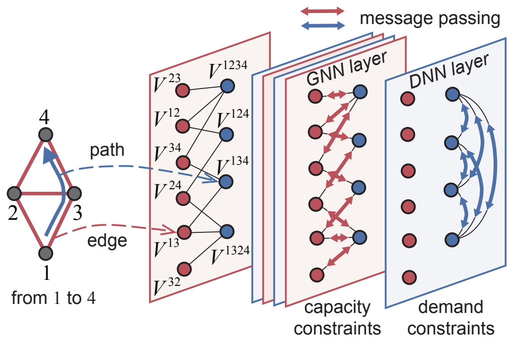

Figure 4: Illustration of a FlowGNN construction. FlowGNN alternates between GNN layers that are designed to capture capacity constraints, and DNN layers that are intended to capture demand constraints.

embeddings learned for each flow of the demand and inputs them into a shared policy (neural) network. The policy network, which allocates demands independently, is trained offline to coordinate flow allocations toward optimizing a global TE objective (e.g., total flow), through a *multi-agent reinforcement learning (RL)* algorithm we customize for TE (§3.3). This design enables processing demands individually rather than the entire traffic matrix at once, making the policy network more compact (in terms of the parameters to learn) and oblivious to the WAN topology size.

So far, the split ratios output by the policy network might still exceed certain link capacity constraints, resulting in dropped traffic and suboptimal TE performance. To mitigate constraint violations and enhance the solution quality, Teal augments the neural networks (FlowGNN and policy network) with 2–5 rapid iterations of a classical constrained optimization algorithm—*alternating direction method of multipliers (ADMM)* (§3.4). During each iteration, ADMM starts from a potentially infeasible TE solution with capacity violations and advances toward the feasible region, fine-tuning traffic splits to meet more constraints and improve the overall TE performance. Each iteration of ADMM is inherently parallel. When warm-started with a reasonably good solution such as the one generated by the neural networks, ADMM can attain a noticeable improvement in performance within several fast iterations.

For each WAN topology, Teal trains its "model"—FlowGNN and policy network—end to end to optimize an operator-provided TE objective; ADMM requires no training. All the three key components of Teal (FlowGNN, multi-agent RL, and ADMM) are carefully designed to be highly parallelizable, enabling fast computation and scalable TE performance as the size of the WAN topology grows.

3.2 Feature learning with FlowGNN

In light of the graph-based structure of WAN topologies, Teal leverages graph neural networks (GNNs) for feature learning. GNNs are a family of neural networks designed to handle graph-structured data [50] and have found applications in various domains, including network planning [71], social network [9, 42], and traffic prediction [36].

GNNs typically store information in graph attributes, commonly in nodes, using a compact vector representation known as *embeddings* [18]. To preserve graph connectivity in the embeddings, neighboring nodes in the GNN exchange information through "message passing" [15]: Each node collects the embeddings from adjacent nodes, transforms the aggregated embeddings using a learned transformation function (e.g., encoded in a fully-connected neural network), and updates its own embedding with the result. GNNs are intrinsically parallel as message passing occurs simultaneously across nodes. Applying message passing once constitutes one GNN layer, and stacking multiple GNN layers allows information to be disseminated multiple hops away. It is noteworthy that GNNs are parameter efficient because each layer shares the same transformation function that operates in the low-dimensional embedding space, which does not grow in proportion to the input graph size.

Despite the strengths of GNNs, the primary focus of TE is the assignment of *flows*, in which each flow originating from a demand follows a predefined *path* along a chain of network links (*edges*). TE is concerned with the interference between flows as they compete for link capacities. Hence, we put a spotlight on flows and explicitly represent flow-related entities—edges and paths—as the nodes in our TE-specific GNN, which we call *FlowGNN*.

Figure 4 exemplifies the construction of a FlowGNN. At a high level, FlowGNN alternates between *GNN layers* aimed at capturing capacity constraints, and *DNN layers* aimed at capturing demand constraints, which dictate that the total volume of all flows derived from a demand should not exceed the demand itself (formal formulation in Appendix A).

The GNN layer in FlowGNN is structured as a bipartite graph. For each edge in the input topology, we create an "EdgeNode" (e.g., V^{13} for the edge connecting nodes #1 and #3), and for each preconfigured path associated with a demand, we create a "PathNode" (e.g., V^{134} for the path containing nodes #1, #3, and #4). An EdgeNode and a PathNode are connected in the GNN layer if and only if the edge lies on the path (e.g., V^{13} is connected to V^{134} but not to V^{124}). The intuition of this setup is to allow EdgeNodes and PathNodes to interact and learn to respect capacity constraints during message passing. For example, when an edge serves as a bottleneck for competing flows, the EdgeNode's embedding will be influenced by its neighboring PathNodes. During initialization, the embedding of an EdgeNode is initialized with the capacity of the corresponding edge, (e.g., V^{13} is initialized to the link capacity between nodes #1 and #3), while the embedding of a PathNode is initialized with the volume of the associated demand (e.g., V^{134} is initialized to the traffic demand from node #1 to node #3). In doing so, a PathNode's embedding becomes dependent on the corresponding demand specified in a traffic matrix, thereby capturing a *flow* routed on the path (rather than the underlying physical network path).

Due to the absence of connections between PathNodes, the GNN layer is unable to make each PathNode aware of the other PathNodes associated with the same demand. To address this, we add a DNN layer after each GNN layer to coordinate flows—represented by their PathNodes—that stem from the same demand. The DNN layer, a fully-connected neural network, essentially transforms and updates the embeddings of the related PathNodes (e.g., V^{1234}, V^{124}, V^{134}, and V^{1324} for the demand from node #1 to node #4). Specifically, these embeddings are fed into the DNN layer to obtain an equal number of updated embeddings, which are then stored back into the respective PathNodes.

Once the FlowGNN is fully trained (in conjunction with the policy network described next), it learns to generate embeddings that encode the graph-structured input of TE in the embedding space. In particular, the final embeddings associated with PathNodes represent the learned feature vectors of flows traversing those paths and serve as informative input for the following task of flow allocation. We visualize the learned flow embeddings in §5.8 to interpret their encoded knowledge about path congestion.

3.3 Flow allocation with multi-agent RL

Given the flow embeddings generated by FlowGNN as feature inputs, TEAL creates a *policy network* to map these embeddings to traffic splits on the corresponding paths, materializing flow allocation. The FlowGNN and policy network constitute the "model" of TEAL, which is trained end to end to optimize an operator-specified TE objective.

Since a network link is frequently utilized by many competing flows, an ideal policy network should process all flows simultaneously to determine the globally optimal allocations. However, this approach entails enormous input and output spaces, resulting in a gigantic neural network with a large number of parameters. To put it in perspective, for a WAN topology with a thousand nodes, the ideal policy network would require *millions of* flow embeddings as input, and output an equal number of split ratios, one for each flow. In practice, we find that this type of gigantic policy network is difficult to train and leads to a significant amount of demand unfulfilled (§5.7).

To reduce the problem dimension and the number of parameters to learn, TEAL processes each demand independently[2] using a shared policy network that is significantly smaller in size (as illustrated in Figure 5). For instance, when assigning a traffic demand across four candidate paths, our policy network only obtains four (low-dimensional) flow embeddings from FlowGNN as input (e.g., the embeddings of V^{1234}, V^{124}, V^{134}, and V^{1324}), and outputs four split ratios to prescribe the allocation. Different demands are processed simultaneously as a batch input to the policy network.

[2]This approach bears resemblance to distributed TE [28], but we target a centralized TE controller with full visibility into the entire WAN topology.

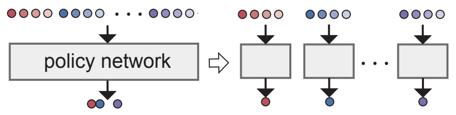

Figure 5: TEAL processes each demand independently using a shared, significantly smaller policy network.

This design allows the policy network to be agnostic to the WAN topology size, making it more compact and feasible to learn.

Despite the benefits, allocating each demand independently can result in a lack of coordination unless the policy network is trained—along with FlowGNN—to be aware of a central TE objective. This raises the question: *What learning algorithm is suitable for training TEAL's model, which generates local traffic splits for each demand while optimizing a global TE objective?* To address this question, we discuss several candidates below before landing on multi-agent RL.

Supervised learning: In an offline setting, LP solvers such as Gurobi can be used to compute the optimal traffic allocations, thereby providing ground-truth traffic splits for TEAL's model to learn using standard supervised learning. Nevertheless, generating these ground-truth labels for large WANs can be excessively time-consuming and incur substantial memory usage. E.g., Gurobi requires 5.5 hours to find the optimal allocations for a single traffic matrix on a 1739-node topology, while consuming up to 18.1 GB of memory.

Direct loss minimization: Supervised learning minimizes the distance between the optimal splits of each demand and the output splits from TEAL's model as the loss. In fact, any *differentiable* loss function can be used instead and minimized directly through gradient descent, referred to as "direct loss minimization" [19, 54]. However, common TE objectives are *non-differentiable*. E.g., calculating the total (feasible) flow requires reconciling flows that collectively exceed a link's capacity, such as by proportionally dropping traffic from each flow. Consequently, the gradient of the total feasible flow with respect to model parameters is zero[3], thus preventing learning through gradient descent. To address this, a common workaround is to approximate the non-differentiable loss function with a differentiable "surrogate loss." In §5.7, we define a surrogate loss that approximates the total feasible flow and implement a baseline to directly minimize this surrogate loss. However, using a surrogate loss entails approximation errors, and identifying a suitable surrogate loss for a different TE objective may not be straightforward.

Multi-agent RL: TEAL opts for employing the framework of multi-agent RL [11, 12, 60], casting the allocation of each demand as an RL agent striving to attain a shared objective in collaboration with other agents. Each agent utilizes locally accessible information, i.e., the flow embeddings of its own demand, to independently generate traffic splits. During training, however, TE allows us to simulate the combined effect of local traffic splits and compute a global TE objective, which serves as an accurate signal, or "reward," to guide the RL agents. The desired TE objective (e.g., the non-differentiable total feasible flow) can be used directly as the reward because RL algorithms do not require a differentiable reward function. Upon the

[3]In this case, we also refer to the loss function as "non-differentiable."

completion of training, each agent executes independently without attending to the other agents. This learning paradigm—centralized training of decentralized policies—is standard in the multi-agent setting when applicable, with COMA [12] being the state of the art. We tailor COMA to TE and implement it in Teal as follows.

Our variant of COMA, referred to as *COMA**, is also based on policy gradients [55], a workhorse of modern deep RL that optimizes a parameterized policy (as encoded in our policy network) with respect to the long-term return (expected cumulative reward). Unlike COMA, our COMA* capitalizes on the fact that the traffic allocations in TE computed for one time interval do not affect future intervals (e.g., traffic matrices). This domain-specific insight allows us to improve training by reducing the long-term return to a one-step return, as well as enhance another key mechanism within COMA (related to the estimation of the reward contributions of individual agents). We include the details of COMA* in Appendix B.

3.4 Solution fine-tuning with ADMM

In essence, TE is a constrained optimization problem, yet neural networks are known to be inadequate in enforcing constraints, such as link capacities in TE. As a result, the traffic allocations directly generated by Teal's neural network model are prone to link overutilization. To mitigate constraint violations and enhance solution quality, Teal fine-tunes the allocation results using 2–5 fast iterations of ADMM (Alternating Direction Method of Multipliers) [5], a classical constrained optimization algorithm.

We outline the mechanism of ADMM below with additional details provided in Appendix C. ADMM is a variant of the augmented Lagrangian method [3], which transforms the original constrained optimization problem into a series of unconstrained problems by converting constraints into penalty terms in the objective function. Applying ADMM in TE optimization requires that we decouple constraints properly and introduce auxiliary variables (a standard optimization technique) for each edge, path, or demand based on the corresponding constraints. Then, in each iteration, ADMM alternates between *i)* minimizing the augmented Lagrangian with respect to one variable while keeping other variables fixed, and *ii)* updating the variables in a manner that balances optimization and constraints.

ADMM is well-suited to Teal for two reasons. First, unlike the widely used optimization methods in LP solvers, such as simplex and interior-point methods, ADMM does not require a constraint-satisfying solution to begin with. Instead, ADMM allows starting from a constraint-violating point (as Teal's neural networks might output) and iteratively moves toward the feasible region. Second, ADMM is highly parallelizable because the minimization of the augmented Lagrangian can be decomposed into many subproblems, each solving for a single variable, e.g., created for each path or edge in TE. These subproblems can be solved in parallel and benefit from significant acceleration on GPUs.

Additionally, we note that using ADMM alone does not accelerate TE optimization. This is because when initialized randomly, ADMM still requires an excessive number of iterations to converge to an acceptable solution, forfeiting its fast speed *within* each iteration. In contrast, Teal's neural networks can warm-start ADMM with a reasonably good solution, allowing ADMM to perform fine-tuning and attain a noticeable improvement in several iterations with a negligible impact on the overall run time.

4 IMPLEMENTATION OF TEAL

Implementing Teal. In each time window (e.g., 5 minutes), Teal takes as input a WAN topology with link capacities, a traffic matrix indicating the demand between every node pair, and 4 precomputed paths to route each demand. The output is 4 split ratios for each demand, prescribing its allocation across the precomputed paths. We implemented all three key modules of Teal in PyTorch. Hyperparameters (e.g., the number of neural network layers) are tuned empirically by testing various values (§5.7).

- *FlowGNN.* FlowGNN comprises 6 GNN layers interleaved with 6 DNN layers. The embeddings in the first GNN layer are initialized as described in §3.2, each with a single element. In each of the following GNN layers, the embedding dimension is expanded by one element, filled with the same value as the original initialization (a technique to enhance the expressiveness of GNNs [44]). The final output embeddings consist of 6 elements each.
- *Multi-agent RL.* The policy network in Teal is implemented as a fully-connected neural network with a single hidden layer of 24 neurons. It has 24 input neurons to receive 4 flow embeddings from FlowGNN for each demand, and uses 4 output neurons, followed by a softmax normalization, to generate 4 split ratios.
- *ADMM.* We apply two iterations of ADMM for topologies with fewer than 100 nodes, and five iterations otherwise.

Training Teal. We train a separate Teal model per WAN topology and per TE objective. The Adam optimizer [29] is employed for stochastic gradient descent, with a learning rate of 10^{-4}. Training Teal from scratch takes approximately a week to complete on large WAN topologies, such as ASN.

Retraining. We retrain Teal if a new node or link is added to the WAN topology permanently. We demonstrate in §5.3 that transient link failures do not require retraining. Compared with training from scratch, each retraining session of Teal only takes 6–10 hours.

5 EVALUATION

In this section, we first describe our evaluation methodology in §5.1. Next, we compare Teal with state-of-the-art TE schemes in §5.2 and show that Teal simultaneously achieves substantial acceleration and near-optimal flow allocation. §5.3 demonstrates Teal's fast reaction to link failures, and §5.4 assesses Teal's robustness to temporal and spatial fluctuations in traffic demands. §5.5 evaluates Teal's flexibility with respect to different TE objectives. §5.6 reports the idealized offline performance of TE schemes disregarding their computation times. Finally, we examine the contributions of Teal's individual components in §5.7, and visualize its learned flow embeddings in §5.8 to interpret its behaviors.

5.1 Methodology

Topologies. We consider five WAN topologies: Google's private WAN (B4 [25]), Microsoft's software-defined WAN (SWAN [21]), two topologies from the Internet Topology Zoo [30]—UsCarrier and Kdl—and an AS-level internet topology [6] adapted for WAN

	# of nodes	# of edges
B4	12	38
SWAN	$O(100)$	$O(100)$
UsCarrier	158	378
Kdl	754	1,790
ASN	1,739	8,558

Table 1: Network topologies in our evaluation.

Algorithm	Computation time
Teal	Total run time (with GPU)
LP-all	Gurobi run time
LP-top	Gurobi run time + model rebuilding time
NCFlow	Gurobi run time + time to coalesce subproblems
POP	Gurobi run time
TEAVAR*	Gurobi run time

Table 2: Breakdown of computation time for each scheme.

purposes, denoted as "ASN." Their numbers of nodes and edges are summarized in Table 1, with additional topology characteristics in Appendix D. We adopt the path formulation of TE used in production (Appendix A), and precompute 4 shortest paths [2, 46] between every pair of nodes as the candidate paths to allocate flows. In cases where link capacities are not provided, we set the capacities to ensure that the best-performing TE scheme satisfies a majority of traffic demand.

Traffic data. We collect traffic data over a 20-day period in 2022 from SWAN, the production inter-datacenter WAN at Microsoft. The total traffic observed in each 5-minute interval between every source-destination pair is considered as their demand. To translate these traffic demands from SWAN to other topologies, we map each new node pair to a random node pair in SWAN, and randomly sample disjoint sequences of traffic matrices, with 700 consecutive intervals for training, 100 for validation, and 200 for testing.

Baselines. We compare Teal against the following baselines.

- *LP-all:* LP-all solves the TE optimization problem for *all* demands using linear programming (LP). Gurobi [17] v9.1.2 is employed as the LP solver.
- *LP-top:* LP-top implements a simple yet effective heuristic TE algorithm that is recently revealed as "demand pinning" [45]. It allocates the top α% of demands using an LP solver and assigns the remaining demands to the shortest paths. To balance allocation quality and computation time, we set $\alpha = 10$ after testing multiple values. In our traffic trace, the top 10% of demands account for a vast majority (88.4%) of the total volume.
- *NCFlow:* NCFlow [2] partitions the topology into disjoint clusters and concurrently solves the subproblem of TE optimization within each cluster using an LP solver. The results obtained from each cluster are then merged in a nontrivial fashion to generate a valid global allocation. We adopt the same number of clusters as specified in the paper for UsCarrier and Kdl, and apply the default partitioning algorithm ("FMPartitioning") for other topologies.
- *POP:* POP [46] replicates the entire topology k times, with each replica having $1/k$ of the original link capacities. The traffic demands are randomly distributed to these replicas, and each subproblem is solved in parallel with an LP solver. We set k based on the topology size, with $k = 1$ for B4 and SWAN, $k = 4$ for UsCarrier, and $k = 128$ for Kdl and ASN. Client splitting threshold is set to 0.25 to break down large demands.
- *TEAVAR*:* TEAVAR [4] is a TE scheme that takes into account the risk of link failures. It balances link utilization with operator-defined availability requirements when allocating traffic. We compare Teal with TEAVAR*, a variant of TEAVAR adapted by NCFlow to maximize the total flow.

Objectives. Our default TE objective is to maximize the total (feasible) flow [2, 21, 25]. Section 5.5 evaluates two additional objectives: minimizing the max link utilization (MLU) [10, 58], and maximizing the total flow with delay penalties [8].

Metrics. We consider the following performance metrics.

- *Computation time:* We measure the total time required by each scheme to compute flow allocation amortized over each traffic matrix, while carefully excluding one-time costs such as the initialization time. The measurement is conducted on 16 CPU threads (Intel Xeon E5-2680) following the setup in NCFlow [2]. An additional GPU (Nvidia Titan RTX) is made available to all schemes, except that only Teal is able to utilize it. Table 2 provides a breakdown of the computation time for each scheme.
- *Satisfied demand:* We focus on the percentage of demand satisfied by a TE scheme in a practical *online* setting [2], accounting for the delay in TE control. This means that the current flow allocation will persist until the TE scheme finishes computing a new allocation. We note that the satisfied demand only normalizes the total flow with respect to the total demand, making it an appropriate metric for evaluating schemes that optimize the total flow.
- *Offline satisfied demand:* We also present the satisfied demand calculated in an idealized *offline* setting in §5.6, where TE schemes are assumed to complete flow allocation instantaneously. This metric eliminates the impact of delay on TE control and focuses solely on the allocation quality.

5.2 Teal vs. the state of the art

Figure 6 compares Teal against the state-of-the-art schemes on four network topologies. Although Teal is not designed for small topologies such as SWAN and UsCarrier, where an LP-solver can also quickly find the optimal allocation, we include the results to demonstrate the trend (note that the computation time in Figure 6a is in log scale). As the network size increases, we observe that Teal demonstrates scalable performance precisely as intended, requiring less than 1 second of computation time while allocating comparable or higher demand on Kdl and ASN. On ASN, for instance, Teal achieves 197–625× speedups relative to the baselines (LP-all is not viable) while satisfying 6–32% more demand.

Small topologies (SWAN and UsCarrier). All the evaluated schemes can compute flow allocation on SWAN and UsCarrier

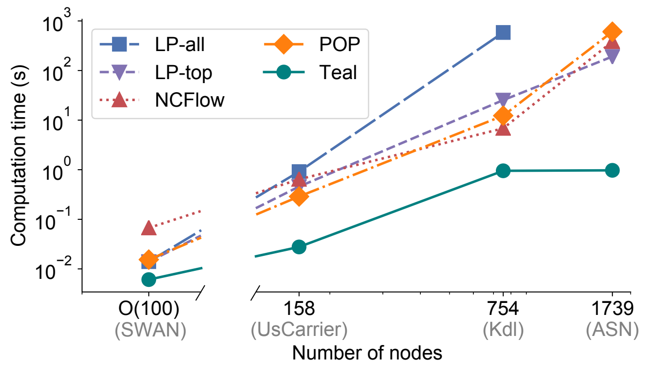

(a) Average computation time

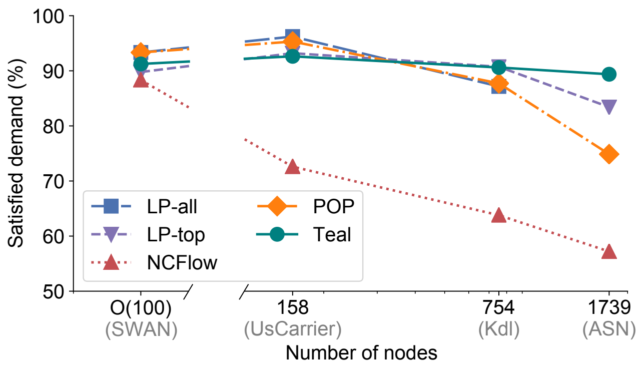

(b) Average satisfied demand

Figure 6: Comparing Teal with LP-all, LP-top, NCFlow, and POP across different networks (LP-all is not feasible on ASN). Designed to accelerate TE optimization on large topologies such as Kdl and ASN, Teal attains scalable performance as the network size grows, reducing computation time to less than 2 seconds while satisfying comparable or higher demand.

within seconds, e.g., LP-all takes less than 1 second to determine the optimal allocation, eliminating the need for TE acceleration schemes. Nonetheless, we observe that when NCFlow is applied to UsCarrier, it can only meet 72.6% of the demand (vs. 96.2% for LP-all). In contrast to its suboptimal performance, Teal retains a demand of 92.6% that is close enough to the optimal.

Kdl. On the larger Kdl topology with 754 nodes and 1,790 edges, Teal takes only 0.95 seconds on average to complete each flow allocation, which is 7× faster than NCFlow, 13× faster than POP, 27× faster than LP-top, and 616× faster than LP-all. Meanwhile, Teal satisfies 90.6% of the demand, nearly the same as the best-performing scheme LP-top (with a difference of only 0.14%). Among the other schemes, LP-all requires over 585 seconds for computation, exceeding the 5-minute time budget and forcing it to reuse stale routes from several intervals ago. As a result, LP-all only allocates 87.2% of the demand despite its ability to find the optimal solution if granted unlimited run time. NCFlow and POP, on the other hand, produce flow allocations quickly as intended, yet they only satisfy 63.8% and 87.7% of the demand, respectively.

ASN. On the largest topology of ASN with 1,739 nodes and 8,558 edges, Teal achieves a more remarkable speedup relative to the other schemes. With an average computation time of 0.97 seconds, Teal is 394× faster than NCFlow, 625× faster than POP, and 197× faster than LP-top. LP-all is impractical to run on ASN due to its incredibly slow computation time of up to 5.5 hours per allocation (4 orders of magnitude slower than Teal), as well as the memory errors incurred. Not only does Teal attain substantial acceleration, it also allocates the most demand on average (89.4%), surpassing LP-top by 6%, POP by 14.5%, and NCFlow by 32%.

Figure 7 zooms in on the performance of schemes on ASN as CDF curves. In Figure 7a, we observe that Teal's computation time remains highly stable across the tested traffic matrices, staying within 0.89–1.08 seconds at all percentiles. This remarkable stability can be attributed to the fact that Teal performs exactly one forward pass on its neural networks, followed by precisely five iterations of ADMM (on this topology). Thus, the amount of computation

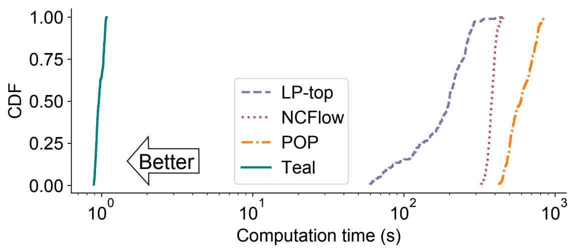

(a) CDF of computation time on ASN

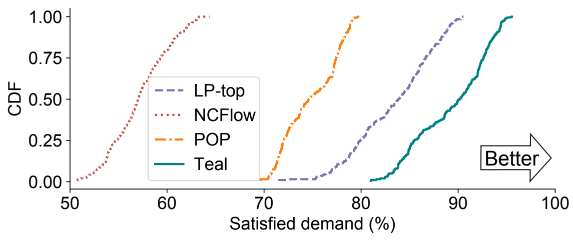

(b) CDF of satisfied demand on ASN

Figure 7: CDFs for the computation time and satisfied demand of schemes on ASN. Teal outperforms the baselines on both dimensions across nearly all percentiles.

(measured in floating-point operations) is independent of the values in the input traffic matrix. By contrast, the computation times of POP, NCFlow, and LP-top fluctuate between 60–839 seconds, e.g., 257–730× slower than Teal at the 90th percentile. The reason for this variability is that the LP solvers employed in these methods have a stopping criterion that is affected by problem-specific factors, such as the ratio between traffic demands and link capacities. Meanwhile, NCFlow involves nontrivial consolidation of the subproblem results, and needs to iterate between LP optimization and consolidation until a predefined accuracy threshold is reached.

Figure 7b shows that TEAL achieves the highest flow allocation across all percentiles. Compared with NCFlow, POP, and LP-top, TEAL's satisfied demand is 6–33% higher at the median, and 5–33% higher at the 90th percentile. We believe that TEAL's robust performance makes it a compelling choice for production TE systems.

5.3 Reacting to link failures

TEAL efficiently solves TE optimization within a second, even for large topologies with thousands of nodes such as ASN. The real-time computation allows TEAL to react promptly to link failures [2], as TEAL can quickly recompute flow allocation on the altered topology (with failed links having zero capacities).

Although TEAVAR* is designed explicitly for fault tolerance under link failures, it is only viable on the small B4 network due to its significant computational overhead. Therefore, we first evaluate all TE schemes on B4 and plot their immediate allocation performance after the introduction of one or two link failures, with no link failures serving as a baseline. Figure 8 shows that as the number of link failures increases, the demand satisfied by all the tested schemes declines as expected. Nevertheless, TEAL consistently outperforms TEAVAR* by 2.4–5.1%, while being statistically indistinguishable from the other schemes. It can be seen that in preparation for potential link failures, TEAVAR* has sacrificed link utilization for higher availability. In contrast, we concur with NCFlow's viewpoint [2]: the performance decline during transient link failures can be compensated through rapid recomputation.

In practice, massive inter-datacenter link failures are very rare. Even with fiber link failures, they do not usually translate to loss of capacity on an inter-datacenter link (unless due to a fiber cut) [53]. As a stress test, however, we evaluate the extreme failure scenarios depicted in prior work [70] and artificially inject 50, 100, and 200 link failures to the ASN network. Figure 9 presents the results for the only 4 schemes feasible on ASN. From the figure, we observe a similar trend across a variety of link failures: TEAL is able to route substantially more traffic demand than the baseline TE schemes, and the ranking is consistent with their run times shown in §5.2. Specifically, TEAL (with a run time less than 1 second) satisfies 6–8% more demand than LP-top (191 s), 15–18% more demand than POP (382 s), and 32–33% more demand than NCFlow (606 s). The reason is that the baseline TE schemes take significantly longer than TEAL to recompute new allocations upon link failures. As a result, thousands of traffic flows have traversed the failed links and been dropped during the computation of rerouting strategies.

It is noteworthy that TEAL achieves the above performance without having to retrain its neural network models, showcasing its generality across (transient) link failures. In the less common event of persistent link failures or planned network upgrades such as new network nodes or links, we anticipate having sufficient time to retrain TEAL within 6–10 hours and recover its allocation performance on the updated topology.

5.4 Robustness to demand changes

We assess the robustness and generalization of TEAL concerning temporal and spatial variations in traffic demands. We do not specifically address massively unforeseen demands because these scenarios pose a lesser concern in cloud WANs, in contrast to ISP

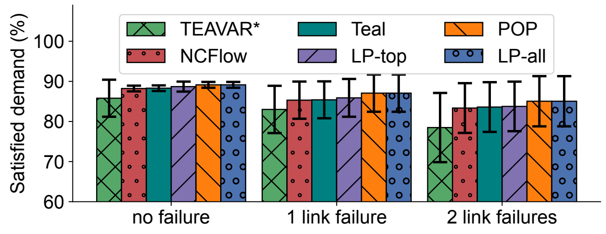

Figure 8: Satisfied demand of TE schemes in the presence of zero, one, or two link failures on the small B4 network. TEAL consistently outperforms TEAVAR* while remaining on par with the other schemes.

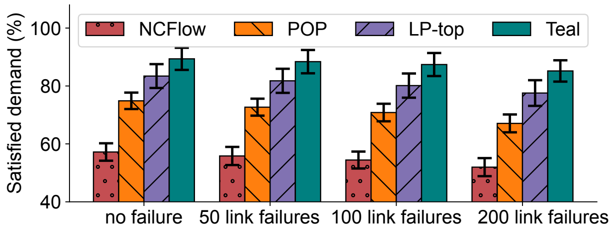

Figure 9: Satisfied demand of TE schemes in the presence of zero, 50, 100, or 200 link failures on the large ASN network. Through fast recomputation, TEAL effectively minimizes the duration impacted by link failures and thus preserves flow allocation performance.

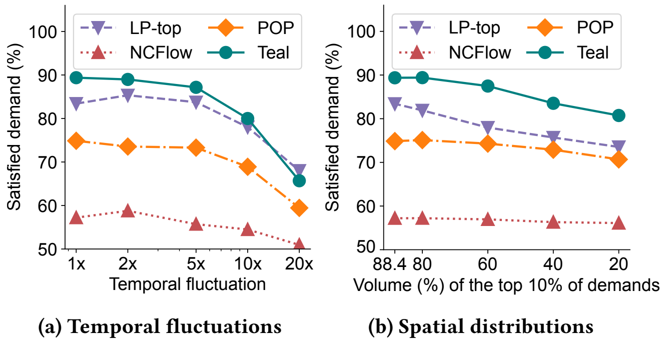

Figure 10: Satisfied demand with temporal and spatial changes.

WANs [61], due to the mitigating effects of bandwidth brokering and TE feedback loop. Nevertheless, in the event that TEAL's performance deteriorates (e.g., in the face of exceptional demand changes), we may concurrently execute an additional TE scheme, such as LP-top, to compute traffic allocation. We can then seamlessly fall back to it if it consistently yields superior solutions than TEAL.

Temporal fluctuation. We introduce various temporal fluctuations to the traffic matrices. For each demand, we calculate the variance in its changes between consecutive time slots, and multiply it by a factor of 2, 5, 10, and 20 to instantiate the variance of a zero-mean normal distribution. Next, we randomly draw a sample from this normal distribution and add it to each demand

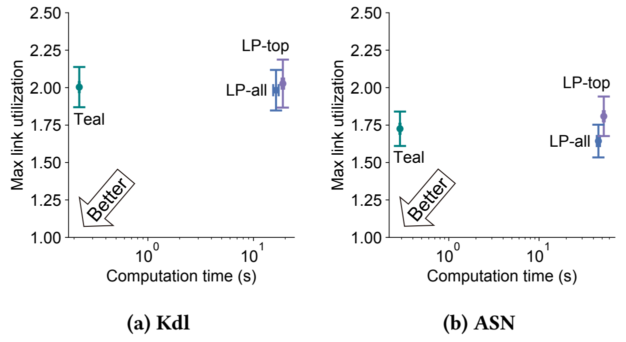

Figure 11: Performance of Teal and baselines under the TE objective of minimizing max link utilization (MLU). All schemes attain comparable MLU, but Teal is 17–36× faster.

in every time slot. Figure 10a shows that almost all the evaluated schemes handle small fluctuations (2× and 5×) effectively, but their performance declines noticeably as the fluctuations escalate to 10× and 20×. Under 10× fluctuation, Teal remains the top performer among all schemes. Under the most severe 20× fluctuation, Teal starts to lag behind LP-top (by 2.3%) due to not seeing the pattern during training, but still outperforms NCFlow and POP by 6–15%.

Spatial distribution. We redistribute traffic demands across node pairs to simulate changes in their spatial distribution. Specifically, we reassign the top 10% of demands, which originally account for 88.4% of the total volume, such that they constitute 80%, 60%, 40%, and 20% instead. As shown in Figure 10b, Teal consistently satisfies the most demand across all spatial distributions. LP-top's performance is reduced by ~10%, as its heuristic is inherently reliant on the heavy-tailed demand distribution.

5.5 Teal under different objectives

In this section, we evaluate the applicability of Teal by retraining it for two different TE objectives: *(i)* minimizing the max link utilization (MLU) [10, 58], and *(ii)* maximizing the latency-penalized total flow [8]. Recall from §3.3 that this is possible due to the flexibility of Teal's RL component with respect to the objective to optimize. Although the above objectives can be transformed into a form compatible with ADMM similarly (as shown in Appendix C), we opt to omit ADMM in these experiments as the neural network model already exhibits satisfactory performance. We compare Teal against LP-all and LP-top since they are directly applicable to the new objectives, which are also linear. However, adapting the codebases of NCFlow and POP to other objectives is challenging, so they are not included in this section.

Max link utilization (MLU). Figure 11 shows that all three schemes yield comparable MLUs, with no statistically significant differences. However, Teal finds a solution within only 0.22–0.29 seconds when minimizing MLU, whereas LP-all and LP-top require 73–85× longer on Kdl and 158–181× longer on ASN. Additionally, we observe two interesting phenomena. First, LP-all and LP-top optimize MLU faster than the total flow, presumably because minimizing MLU is "easier" and requires fewer iterations for convergence in Gurobi. Second, LP-all runs slightly faster than LP-top.

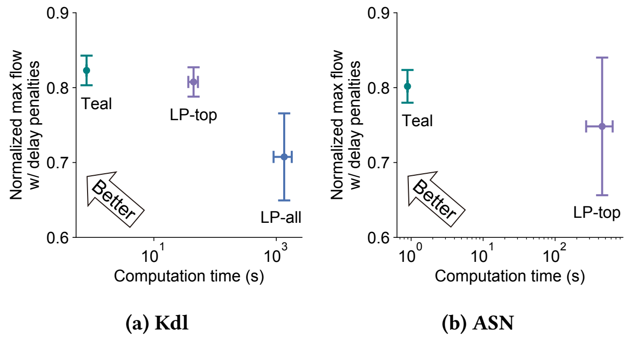

Figure 12: Performance of Teal and baselines under the TE objective of maximizing the total flow with delay penalties (LP-all is not feasible on ASN). Teal achieves the best allocation performance while being 26–718× faster.

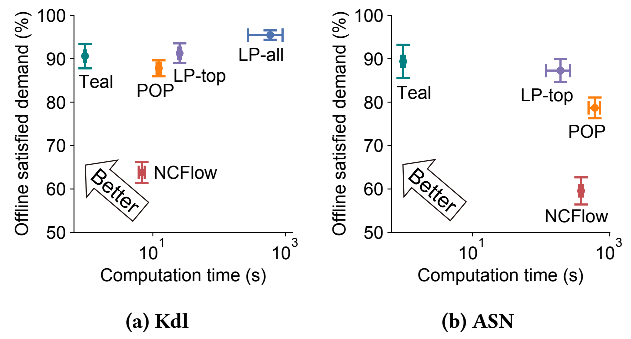

Figure 13: Comparing the offline satisfied demand (defined in §5.1) of Teal with baselines (LP-all is not feasible on ASN). Teal's allocation quality remains close to optimal even when the computational delay is not taken into account.

The reason is that the top 10% of demands vary over time and thus require LP-top to constantly rebuild its model in Gurobi (see Table 2) incurring additional computational overhead.

Latency-penalized total flow. As shown in Figure 12, Teal's solution quality is comparable to or higher than the best-performing scheme LP-top, while being 56–505× faster in speed. LP-all is not feasible on ASN when optimizing for this objective, while being several orders of magnitude (1693×) slower than Teal on Kdl.

5.6 Offline TE performance

To determine the extent to which Teal's performance benefits arise from its fast and scalable computation, we evaluate all schemes under the offline setting described in §5.1.

On Kdl, while LP-all requires over 500 seconds to compute each flow allocation and exceeds the allotted time budget, its output allocation is optimal and serves as a benchmark. Teal falls short of the optimal allocation by 4.8% with respect to the offline satisfied demand, but remains within 0.7% of the best feasible scheme LP-top, and outperforms NCFlow by a significant margin of 27% and POP by 2.8%, respectively. On ASN, Teal and LP-top achieve a similar

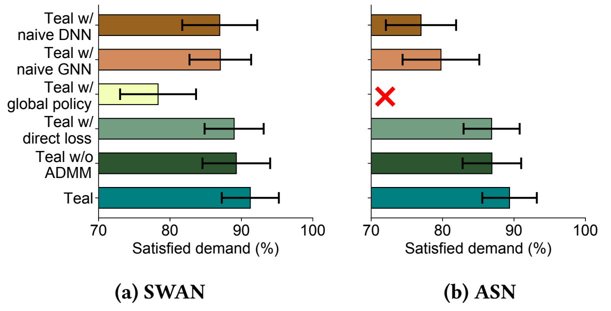

Figure 14: Ablation study of Teal's key features in its FlowGNN, multi-agent RL, and ADMM components. Each feature proves useful for Teal's allocation performance.

level of offline satisfied demand, which is 30% higher than NCFlow and 11% higher than POP.

These findings suggest that even when the computational delay in TE control is not taken into account, Teal's flow allocation quality is still close to optimal. However, we note the caveat that Teal achieves this by essentially "overfitting" the WAN topology, link capacities, and demand distribution. For example, when faced with significant out-of-distribution demands (as shown in §5.4), the knowledge learned by Teal may struggle to apply and maintain the allocation performance.

5.7 Ablation study of Teal

We perform an ablation study to assess the impact of Teal's key features on its overall performance.

Design of FlowGNN. We devise two alternative designs for FlowGNN. The first design, called "Teal w/ naive DNN," employs a 6-layer fully-connected neural network that directly takes a traffic matrix as input and outputs traffic splits. The second, called "Teal w/ naive GNN," models the WAN topology as a GNN directly, with each node in the GNN representing a network site in the WAN for feature learning. This design enables information exchange among neighboring nodes in the WAN, but fails to capture the relationship between edges and paths, or network flows at the path level. Figure 14 reveals that compared with Teal, these two variants allocate 4.2–4.3% less demand on SWAN and 9.6–12.4% on ASN, accentuating the importance of FlowGNN.

Processing demands independently. In contrast to Teal's independent allocation of each demand, an alternate approach described in §3.3 involves processing all demands at once using a "gigantic policy network." This variant, referred to as "Teal w/ global policy," is not feasible for large networks such as ASN due to memory errors. On the smaller SWAN network, it allocates 12.9% less demand on average compared with the full-fledged Teal (Figure 14a).

Use of multi-agent RL. As discussed in §3.3, Teal's multi-agent RL policy can be replaced with direct loss minimization if a non-differentiable TE objective is approximated by a surrogate loss. For the total (feasible) flow, we define a surrogate loss as the total intended flow (ignoring link capacities) minus the total overused capacities (formal definition is in Appendix A). This variant, denoted as "Teal w/ direct loss," allocates 2.3–2.5% less demand on average (Figure 14), presumably due to the approximation error in the surrogate loss. Moreover, Teal's multi-agent RL policy may optimize a flexible array of TE objectives (§5.5), while it is nontrivial to identify a good surrogate loss for a new objective.

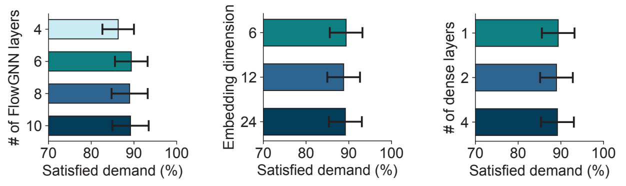

Figure 15: Sensitivity analysis of Teal's hyperparameters.

Fine-tuning with ADMM. Removing ADMM from Teal's pipeline results in a decline of 2–2.5% in the satisfied demand, as indicated by "Teal w/o ADMM" (Figure 14). Although the impact is tolerable, ADMM is a transparent optimization algorithm that strictly reduces constraint violations when applied, fine-tuning the solution with negligible run-time overhead. We believe these properties make ADMM a desirable option for WAN operators.

Sensitivity analysis. We further conduct an analysis on the sensitivity of Teal's performance with respect to its hyperparameters. While the analysis is performed on the ASN topology, similar results are observed across other topologies. Figure 15a depicts the impact of varying the number of layers in FlowGNN. As the number of layers increases from 4 to 6, Teal's satisfied demand rises from 86.3% to 89.4%, with diminishing returns beyond 6 layers. Additionally, we explore different embedding dimensions in FlowGNN. Instead of having a final output embedding of 6 elements (by incrementing the embedding dimension by one in each FlowGNN layer), we also test higher final embedding dimensions such as 12 and 24. However, the improvements achieved with higher embedding dimensions are marginal, as indicated by Figure 15b.

In Figure 15c, we vary the number of fully-connected (dense) layers in the policy network of Teal's multi-agent RL, and observe little difference in the allocation quality. This outcome aligns with our expectations since FlowGNN already captures the complex capacity-demand relationship within its architecture. As a result, multi-agent RL primarily focuses on the task of transforming embeddings into split ratios, requiring only a lightweight structure.

5.8 Visualization of flow embeddings

To gain insights into the behaviors of Teal, we visualize the flow embeddings learned by FlowGNN for the SWAN topology through a technique known as t-SNE (t-distributed stochastic neighbor embedding) [20]. The resulting visualization is shown in Figure 16, where the flow embeddings are projected onto a 2-dimensional space by t-SNE. We color-code each flow embedding based on whether its corresponding path is supposed to be "busy" in an optimal scenario, i.e., it is assigned the largest split ratio among the preconfigured paths in an optimal allocation generated by LP-all.

From the visualization, we observe an orange cluster of busy paths, which is a useful indicator for the subsequent allocation task as the downstream policy network can be trained to separate

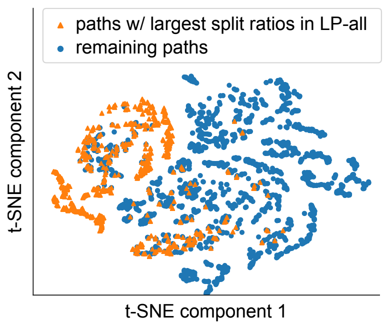

Figure 16: Visualization of embeddings in FlowGNN.

this cluster from the remaining paths and allocate more traffic to the paths desired to be busy, thereby mimicking the optimal solution provided by LP-all. In other words, this cluster indicates that FlowGNN has roughly captured path congestion within the network in its learned embeddings.

However, it is noteworthy that Figure 16 also contains a small number of outliers. This is because TE optimization can yield multiple optimal (or near-optimal) solutions. As a result, the solution generated by Teal might not be identical to that produced by LP-all, leading to the discrepancy between the two approaches.

6 RELATED WORK

TE has been an integral part of service and cloud provider networks. Network operators have leveraged TE to maximize network utilization, guarantee fairness among flows, and prevent link overutilization. While ISPs used switch-native protocols (e.g., MPLS, OSPF) to engineer traffic in their networks [13, 64], cloud providers implemented centralized software-defined TE systems to explicitly optimize for desirable network characteristics, such as low latency, high throughput, and failure resilience [4, 21, 22, 25, 33, 38, 68]. In this section, we place Teal in the context of related work on cloud WAN TE.

Intra-WAN traffic engineering. In the last decade, large cloud providers have deployed SDN-based centralized TE in their planet-scale WANs to allocate traffic between datacenters [21, 25, 33]. Centralized TE systems formulate the problem of allocating traffic in the WAN as an optimization problem and periodically solve it to compute flow allocations. Due to the increase in the scale of WANs and traffic matrices, the time required to solve the optimization problem has become a bottleneck in the TE control loop. Researchers have proposed techniques that solve the TE optimization on smaller subsets of the problem and combine the solutions to compute traffic allocations for the global graph [2, 46]. Teal tackles the scalability challenges faced by modern intra-WAN TE controllers using a learning-based approach.

Inter-WAN traffic engineering. Cloud providers engineer traffic at the edge of their networks by allocating demands on the links between the cloud and ISPs. Recent work has shown the role of engineering inter-WAN traffic for performance improvement and cost reduction [51, 52]. In contrast, Teal focuses on intra-WAN TE.

ML for traffic engineering. Deep learning and broader ML techniques have seen applications in a range of classical networking problems, including adaptive video streaming [41, 66], TCP congestion control [26, 67], and traffic demand prediction [35, 40]. Recently, researchers have begun leveraging ML to allocate traffic in WANs [49, 58, 59], focusing on learning to route under traffic uncertainty and exploiting the predictive power of ML to improve allocation performance. However, production WAN TE still heavily relies on separate components such as bandwidth brokers to provide the traffic matrix for the next TE time step as input to the TE controller. Other ML-based approaches to TE [14, 39, 43, 65, 69] operate under a variety of assumptions and do not apply to the acceleration of large-scale intra-WAN TE. Our work demonstrates that learning-based approaches can significantly accelerate TE optimization while achieving near-optimal allocation performance, addressing the increasing scale of TE optimization.

7 CONCLUSION

In this work, we demonstrate that deep learning is an effective tool for scaling cloud WAN TE systems to large WAN topologies. We develop Teal, a learning-based TE scheme that combines carefully designed, highly parallelizable components—FlowGNN, multi-agent RL, and ADMM—to allocate traffic in WANs. Teal computes near-optimal traffic allocations with substantial acceleration over state-of-the-art TE schemes for large WAN topologies.

Ethics: This work does not raise any ethical issues.

ACKNOWLEDGMENTS

We thank our anonymous reviewers for their insightful comments and Zhizhen Zhong for shepherding this work. We also thank Srikanth Kandula, Firas Abuzaid, Yang Zhou, Deepak Narayanan, Fiodar Kazhamiaka, Umesh Krishnaswamy, and Victor Bahl for their helpful feedback. This work was supported in part by the NSF grant CNS-2107078.

REFERENCES

[1] Parallelism in LP and MIP, August 2020. https://cdn.gurobi.com/wp-content/uploads/2020/08/How-to-Exploit-Parallelism-in-Linear-and-Mixed-Integer-Programming.pdf.
[2] Firas Abuzaid, Srikanth Kandula, Behnaz Arzani, Ishai Menache, Matei Zaharia, and Peter Bailis. Contracting Wide-area Network Topologies to Solve Flow Problems Quickly. In *Proceedings of USENIX NSDI*, pages 175–200, 2021.
[3] Dimitri P. Bertsekas. *Constrained Optimization and Lagrange Multiplier Methods*. Academic press, 2014.
[4] Jeremy Bogle, Nikhil Bhatia, Manya Ghobadi, Ishai Menache, Nikolaj Bjørner, Asaf Valadarsky, and Michael Schapira. TEAVAR: Striking the Right Utilization-Availability Balance in WAN Traffic Engineering. In *Proceedings of ACM SIGCOMM*. ACM, 2019.
[5] Stephen Boyd, Neal Parikh, Eric Chu, Borja Peleato, Jonathan Eckstein, et al. Distributed Optimization and Statistical Learning Via the Alternating Direction Method of Multipliers. *Foundations and Trends® in Machine learning*, 3(1):1–122, 2011.
[6] CAIDA. The CAIDA AS Relationships Dataset, 2022.
[7] Sharan Chetlur, Cliff Woolley, Philippe Vandermersch, Jonathan Cohen, John Tran, Bryan Catanzaro, and Evan Shelhamer. cuDNN: Efficient Primitives for Deep Learning. *arXiv preprint arXiv:1410.0759*, 2014.
[8] Anwar Elwalid, Cheng Jin, Steven Low, and Indra Widjaja. MATE: MPLS Adaptive Traffic Engineering. In *Proceedings of IEEE INFOCOM*, volume 3, pages 1300–1309 vol.3, 2001.
[9] Wenqi Fan, Yao Ma, Qing Li, Yuan He, Eric Zhao, Jiliang Tang, and Dawei Yin. Graph Neural Networks for Social Recommendation. In *International world Wide Web Conference*, pages 417–426, 2019.
[10] Lisa K. Fleischer. Approximating Fractional Multicommodity Flow Independent of the Number of Commodities. *SIAM Journal on Discrete Mathematics*, 13(4):505–520, 2000.
[11] Jakob Foerster, Ioannis Alexandros Assael, Nando De Freitas, and Shimon Whiteson. Learning to Communicate with Deep Multi-Agent Reinforcement Learning. *Advances in Neural Information Processing Systems*, 29, 2016.
[12] Jakob Foerster, Gregory Farquhar, Triantafyllos Afouras, Nantas Nardelli, and Shimon Whiteson. Counterfactual Multi-Agent Policy Gradients. In *Proceedings of AAAI conference on artificial intelligence*, volume 32, 2018.
[13] Bernard Fortz, Jennifer Rexford, and Mikkel Thorup. Traffic Engineering with Traditional IP Routing Protocols. *IEEE Communications Magazine*, 40(10):118–124, 2002.
[14] Nan Geng, Mingwei Xu, Yuan Yang, Chenyi Liu, Jiahai Yang, Qi Li, and Shize Zhang. Distributed and Adaptive Traffic Engineering with Deep Reinforcement Learning. In *Proceedings of IEEE/ACM International Symposium on Quality of Service (IWQOS)*, pages 1–10, 2021.
[15] Justin Gilmer, Samuel S. Schoenholz, Patrick F. Riley, Oriol Vinyals, and George E. Dahl. Neural Message Passing for Quantum Chemistry. In *International Conference on Machine Learning*, pages 1263–1272. PMLR, 2017.
[16] Google Cloud. Cloud Tensor Processing Units (TPUs), 2022.
[17] Gurobi Optimization, LLC. Gurobi Optimizer Reference Manual, 2022.
[18] William L. Hamilton, Rex Ying, and Jure Leskovec. Representation Learning on Graphs: Methods and Applications. *arXiv preprint arXiv:1709.05584*, 2017.
[19] Tamir Hazan, Joseph Keshet, and David McAllester. Direct Loss Minimization for Structured Prediction. *Advances in Neural Information Processing Systems*, 23, 2010.
[20] Geoffrey E. Hinton and Sam Roweis. Stochastic neighbor embedding. *Advances in Neural Information Processing Systems*, 15, 2002.
[21] Chi-Yao Hong, Srikanth Kandula, Ratul Mahajan, Ming Zhang, Vijay Gill, Mohan Nanduri, and Roger Wattenhofer. Achieving High Utilization with Software-Driven WAN. *ACM SIGCOMM Computer Communication Review*, 43(4):15–26, August 2013.
[22] Chi-Yao Hong, Subhasree Mandal, Mohammad A. Alfares, Min Zhu, Rich Alimi, Kondapa Naidu Bollineni, Chandan Bhagat, Sourabh Jain, Jay Kaimal, Jeffrey Liang, Kirill Mendelev, Steve Padgett, Faro Thomas Rabe, Saikat Ray, Malveeka Tewari, Matt Tierney, Monika Zahn, Jon Zolla, Joon Ong, and Amin Vahdat. B4 and After: Managing Hierarchy, Partitioning, and Asymmetry for Availability and Scale in Google's Software-Defined WAN. In *Proceedings of ACM SIGCOMM*, 2018.
[23] IBM. CPLEX Optimizer, 2022.
[24] GPU-Based Deep Learning Inference and Based Deep Learning. A Performance and Power Analysis. *Nvidia Whitepaper, Nov*, 2015.
[25] Sushant Jain, Alok Kumar, Subhasree Mandal, Joon Ong, Leon Poutievski, Arjun Singh, Subbaiah Venkata, Jim Wanderer, Junlan Zhou, Min Zhu, et al. B4: Experience with A Globally-Deployed Software Defined WAN. *ACM SIGCOMM Computer Communication Review*, 43(4):3–14, 2013.
[26] Nathan Jay, Noga Rotman, Brighten Godfrey, Michael Schapira, and Aviv Tamar. A Deep Reinforcement Learning Perspective on Internet Congestion Control. In *International Conference on Machine Learning*, pages 3050–3059. PMLR, 2019.
[27] Yangqing Jia, Evan Shelhamer, Jeff Donahue, Sergey Karayev, Jonathan Long, Ross Girshick, Sergio Guadarrama, and Trevor Darrell. Caffe: Convolutional Architecture for Fast Feature Embedding. In *Proceedings of the 22nd ACM international conference on Multimedia*, pages 675–678, 2014.
[28] Srikanth Kandula, Dina Katabi, Bruce Davie, and Anna Charny. Walking the Tightrope: Responsive Yet Stable Traffic Engineering. *ACM SIGCOMM Computer Communication Review*, 35(4):253–264, 2005.
[29] Diederik P. Kingma and Jimmy Ba. Adam: A Method for Stochastic Optimization. *arXiv preprint arXiv:1412.6980*, 2014.
[30] Simon Knight, Hung X. Nguyen, Nickolas Falkner, Rhys Bowden, and Matthew Roughan. The Internet Topology Zoo. *IEEE Journal on Selected Areas in Communications*, 29(9):1765–1775, 2011.
[31] Vijay Konda and John Tsitsiklis. Actor-Critic Algorithms. *Advances in Neural Information Processing Systems*, 12, 1999.
[32] Mario Köppen. The Curse of Dimensionality. In *Proceedings of Online World Conference on Soft Computing in Industrial Applications (WSC)*, volume 1, pages 4–8, 2000.
[33] Umesh Krishnaswamy, Rachee Singh, Nikolaj Bjørner, and Himanshu Raj. Decentralized Cloud Wide-Area Network Traffic Engineering with BLASTSHIELD. In *Proceedings of USENIX NSDI*, pages 325–338, Renton, WA, April 2022. USENIX Association.
[34] Umesh Krishnaswamy, Rachee Singh, Paul Mattes, Paul-Andre C. Bissonnette, Nikolaj Bjørner, Zahira Nasrin, Sonal Kothari, Prabhakar Reddy, John Abeln, Srikanth Kandula, et al. OneWAN Is Better than Two: Unifying a Split WAN Architecture. In *20th USENIX Symposium on Networked Systems Design and Implementation (NSDI 23)*, pages 515–529, 2023.
[35] Jitendra Kumar and Ashutosh Kumar Singh. Cloud Resource Demand Prediction Using Differential Evolution Based Learning. In *Proceedings of IEEE International Conference on Smart Computing & Communications (ICSCC)*, pages 1–5. IEEE, 2019.
[36] Oliver Lange and Luis Perez. Traffic Prediction with Advanced Graph Neural Networks, 2020.
[37] Jay Yoon Lee, Michael L. Wick, Jean-Baptiste Tristan, and Jaime G. Carbonell. Enforcing Output Constraints via SGD: A Step Towards Neural Lagrangian Relaxation. In *Proceedings of NeurIPS Workshop on Automated Knowledge Base Construction (AKBC)*, 2017.
[38] Hongqiang Harry Liu, Srikanth Kandula, Ratul Mahajan, Ming Zhang, and David Gelernter. Traffic Engineering with Forward Fault Correction. In Fabián E. Bustamante, Y. Charlie Hu, Arvind Krishnamurthy, and Sylvia Ratnasamy, editors, *Proceedings of ACM SIGCOMM*, pages 527–538. ACM, 2014.
[39] Libin Liu, Li Chen, Hong Xu, and Hua Shao. Automated Traffic Engineering in SD-WAN: Beyond Reinforcement Learning. In *IEEE INFOCOM WKSHPS Workshops*, pages 430–435, 2020.
[40] Tanwi Mallick, Mariam Kiran, Bashir Mohammed, and Prasanna Balaprakash. Dynamic Graph Neural Network for Traffic Forecasting in Wide Area Networks. In *Proceedings of IEEE International Conference on Big Data (Big Data)*, pages 1–10. IEEE, 2020.
[41] Hongzi Mao, Ravi Netravali, and Mohammad Alizadeh. Neural Adaptive Video Streaming with Pensieve. In *Proceedings of ACM SIGCOMM*, pages 197–210, 2017.
[42] Abduallah Mohamed, Kun Qian, Mohamed Elhoseiny, and Christian Claudel. Social-STGCNN: A Social Spatio-Temporal Graph Convolutional Neural Network for Human Trajectory Prediction. In *Proceedings of IEEE/CVF CVPR*, pages 14424–14432, 2020.
[43] Bashir Mohammed, Mariam Kiran, and Nandini Krishnaswamy. DeepRoute on Chameleon: Experimenting with Large-Scale Reinforcement Learning and SDN on Chameleon Testbed. In *Proceedings of IEEE International Conference on Network Protocols (ICNP)*, pages 1–2, 2019.
[44] Vinod Nair, Sergey Bartunov, Felix Gimeno, Ingrid von Glehn, Pawel Lichocki, Ivan Lobov, Brendan O'Donoghue, Nicolas Sonnerat, Christian Tjandraatmadja, Pengming Wang, et al. Solving Mixed Integer Programs Using Neural Networks. *arXiv preprint arXiv:2012.13349*, 2020.
[45] Pooria Namyar, Behnaz Arzani, Ryan Beckett, Santiago Segarra, Himanshu Raj, and Srikanth Kandula. Minding the Gap Between Fast Heuristics and Their Optimal Counterparts. In *Proceedings of the 21st ACM Workshop on Hot Topics in Networks*, pages 138–144, 2022.
[46] Deepak Narayanan, Fiodar Kazhamiaka, Firas Abuzaid, Peter Kraft, Akshay Agrawal, Srikanth Kandula, Stephen Boyd, and Matei Zaharia. Solving Large-Scale Granular Resource Allocation Problems Efficiently with POP. In *Proceedings of ACM SOSP*, pages 521–537, 2021.
[47] John C. Nash. The (Dantzig) Simplex Method for Linear Programming. *Computing in Science and Engg.*, 2(1):29–31, jan 2000.
[48] Adam Paszke, Sam Gross, Francisco Massa, Adam Lerer, James Bradbury, Gregory Chanan, Trevor Killeen, Zeming Lin, Natalia Gimelshein, Luca Antiga, et al. PyTorch: An Imperative Style, High-Performance Deep Learning Library. In *Advances in Neural Information Processing Systems*, pages 8024–8035, 2019.
[49] Yarin Perry, Felipe Vieira Frujeri, Chaim Hoch, Srikanth Kandula, Ishai Menache, Michael Schapira, and Aviv Tamar. DOTE: Rethinking (Predictive) Wan Traffic Engineering. In *20th USENIX Symposium on Networked Systems Design and*

Implementation (NSDI 23), pages 1557–1581, 2023.

[50] Benjamin Sanchez-Lengeling, Emily Reif, Adam Pearce, and Alexander B. Wiltschko. A Gentle Introduction to Graph Neural Networks. *Distill*, 2021. https://distill.pub/2021/gnn-intro.

[51] Brandon Schlinker, Hyojeong Kim, Timothy Cui, Ethan Katz-Bassett, Harsha V Madhyastha, Italo Cunha, James Quinn, Saif Hasan, Petr Lapukhov, and Hongyi Zeng. Engineering Egress with Edge Fabric: Steering Oceans of Content to the World. In *Proceedings of ACM SIGCOMM*, pages 418–431. ACM, 2017.

[52] Rachee Singh, Sharad Agarwal, Matt Calder, and Paramvir Bahl. Cost-Effective Cloud Edge Traffic Engineering With Cascara. In *Proceedings of USENIX NSDI*, pages 201–216, 2021.

[53] Rachee Singh, Manya Ghobadi, Klaus-Tycho Foerster, Mark Filer, and Phillipa Gill. RADWAN: Rate Adaptive Wide Area Network. In *Proceedings of ACM SIGCOMM*, page 547–560, New York, NY, USA, 2018. Association for Computing Machinery.

[54] Yang Song, Alexander Schwing, Raquel Urtasun, et al. Training Deep Neural Networks via Direct Loss Minimization. In *International Conference on Machine Learning*, pages 2169–2177. PMLR, 2016.

[55] Richard S. Sutton, David McAllester, Satinder Singh, and Yishay Mansour. Policy Gradient Methods for Reinforcement Learning with Function Approximation. *Advances in Neural Information Processing Systems*, 12, 1999.

[56] Tensorflow. An End-to-End Open Source Machine Learning Platform, 2022.

[57] The Linux Foundation. Open Neural Network Exchange, 2022.

[58] Asaf Valadarsky, Michael Schapira, Dafna Shahaf, and Aviv Tamar. Learning to Route. In *Proceedings of ACM HotNets*, pages 185–191, 2017.

[59] Asaf Valadarsky, Michael Schapira, Dafna Shahaf, and Aviv Tamar. Learning to route with deep RL. In *NIPS Deep Reinforcement Learning Symposium*, 2017.

[60] Oriol Vinyals, Igor Babuschkin, Wojciech M. Czarnecki, Michaël Mathieu, Andrew Dudzik, Junyoung Chung, David H. Choi, Richard Powell, Timo Ewalds, Petko Georgiev, et al. Grandmaster Level in StarCraft II Using Multi-Agent Reinforcement Learning. *Nature*, 575(7782):350–354, 2019.

[61] Hao Wang, Haiyong Xie, Lili Qiu, Yang Richard Yang, Yin Zhang, and Albert Greenberg. COPE: Traffic Engineering in Dynamic Networks. In *Proceedings of the 2006 conference on Applications, technologies, architectures, and protocols for computer communications*, pages 99–110, 2006.

[62] David H. Wolpert and Kagan Tumer. Optimal Payoff Functions for Members of Collectives. In *Modeling Complexity in Economic and Social Systems*, pages 355–369. World Scientific, 2002.

[63] Zonghan Wu, Shirui Pan, Fengwen Chen, Guodong Long, Chengqi Zhang, and S. Yu Philip. A Comprehensive Survey on Graph Neural Networks. *IEEE transactions on neural networks and learning systems*, 32(1):4–24, 2020.

[64] Xipeng Xiao, A. Hannan, B. Bailey, and L. M. Ni. Traffic Engineering with MPLS in the Internet. *IEEE Network*, 14(2):28–33, March 2000.

[65] Zhiyuan Xu, Jian Tang, Jingsong Meng, Weiyi Zhang, Yanzhi Wang, Chi Harold Liu, and Dejun Yang. Experience-Driven Networking: A Deep Reinforcement Learning Based Approach. *CoRR*, abs/1801.05757, 2018.

[66] Francis Y. Yan, Hudson Ayers, Chenzhi Zhu, Sadjad Fouladi, James Hong, Keyi Zhang, Philip Levis, and Keith Winstein. Learning *in Situ*: A Randomized Experiment in Video Streaming. In *Proceedings of USENIX NSDI*, pages 495–511, Santa Clara, CA, February 2020. USENIX Association.

[67] Francis Y. Yan, Jestin Ma, Greg D. Hill, Deepti Raghavan, Riad S. Wahby, Philip Levis, and Keith Winstein. Pantheon: the Training Ground for Internet Congestion-Control Research. In *Proceedings of USENIX ATC*, pages 731–743, Boston, MA, July 2018. USENIX Association.

[68] Kok-Kiong Yap, Murtaza Motiwala, Jeremy Rahe, Steve Padgett, Matthew Holliman, Gary Baldus, Marcus Hines, Taeeun Kim, Ashok Narayanan, Ankur Jain, et al. Taking the Edge off with Espresso: Scale, Reliability and Programmability for Global Internet Peering. In *Proceedings of ACM SIGCOMM*, pages 432–445, 2017.

[69] Junjie Zhang, Minghao Ye, Zehua Guo, Chen-Yu Yen, and H. Jonathan Chao. CFR-RL: Traffic Engineering with Reinforcement Learning in SDN. *IEEE Journal on Selected Areas in Communications*, 38(10):2249–2259, 2020.

[70] Zhizhen Zhong, Manya Ghobadi, Alaa Khaddaj, Jonathan Leach, Yiting Xia, and Ying Zhang. ARROW: Restoration-Aware Traffic Engineering. In *Proceedings of ACM SIGCOMM*, page 560–579, New York, NY, USA, 2021. Association for Computing Machinery.

[71] Hang Zhu, Varun Gupta, Satyajeet Singh Ahuja, Yuandong Tian, Ying Zhang, and Xin Jin. Network Planning with Deep Reinforcement Learning. In *Proceedings of ACM SIGCOMM*, pages 258–271, 2021.

Appendices

Appendices are supporting material that has not been peer-reviewed.

A TE OPTIMIZATION FORMULATION

The goal of cloud WAN traffic engineering (TE) algorithms is to efficiently utilize the expensive network resources between datacenters to achieve operator-defined performance goals, such as minimum latency, maximum throughput, and fairness between customer traffic flows.

Network. We represent the WAN topology as a graph $G = (V, E, c)$, where nodes (V) represent network sites (e.g., datacenters), edges (E) between the sites represent network links resulting from long-haul fiber connectivity, and $c : E \longrightarrow \mathbb{R}^+$ assigns capacities to links. Let $n = |V|$ denote the number of network sites. Each network site can consist of either one or multiple aggregated routers.

Traffic demands. The demand $d \in D$ between a pair of network sites s and t in G is the volume of network traffic originating from s that must be routed to t within a given duration of time. A separate component in the system (such as a bandwidth broker) periodically gauges demands for the next time interval (e.g., five minutes) based on the needs of various services, historical demands, and bandwidth enforcement [25]. The gauged demand is considered fixed for the next time interval and provides as input to the TE optimization. The TE algorithm computes allocations along network paths to meet the given demand [2, 58].

Network paths. The network traffic corresponding to a demand d flows on a set of preconfigured network paths P_d. These paths are precomputed by network operators (e.g., using the shortest paths) and serve as input to the TE optimization. This version of TE optimization that allocates demands onto preconfigured paths as opposed to individual edges, is known as the path formulation of TE, which is widely adopted in production WANs [21, 22, 25, 33]. Path formulation reduces the computational complexity of the TE optimization and also reduces the number of switch forwarding entries required to implement the traffic allocation.

Traffic allocations. A traffic allocation $\mathcal{F}$ allocates a demand $d \in D$ as flows across the assigned network paths P_d. Therefore, $\mathcal{F}_d$ is a mapping from the path set P_d to non-negative split ratios, i.e., $\mathcal{F}_d : P_d \longrightarrow [0, 1]$, such that $\mathcal{F}_d(p)$ is the fraction of traffic demand d allocated on path p. The traffic allocation in time interval i is denoted as $\mathcal{F}^{(i)}$.

Constraints. For any demand $d \in D$, $\sum_{p \in P_d} \mathcal{F}_d(p) \leq 1$ is maintained such that we only allocate as much traffic as the demands. Additionally, we constrain the allocations by $e \in E$, $c(e) \geq \sum_{p \ni e} \sum_{d \in D} \mathcal{F}_d(p) \cdot d$ to ensure that the traffic allocations do not exceed the capacity of network links.

TE objectives. The goal of TE algorithms can range from maximizing network throughput to minimizing latency, and previous work has explored algorithms with a variety of TE objectives. We show that TEAL can achieve near-optimal allocation with substantial acceleration for different well-known TE objectives (§5). In this section, we illustrate the TE optimization problem using the maximum network flow objective since it has been adopted by production TE systems [21, 33]. The TE optimization computes a routing policy $\mathcal{F}$ that satisfies the demand and capacity constraints while maximizing the TE objective. Equation (1) summarizes our TE formulation:

$$\begin{aligned} \text{maximize} \quad & \sum_{d\in D}\sum_{p\in P_d} \mathcal{F}_d(p)\cdot d \\ \text{subject to} \quad & \sum_{p\in P_d} \mathcal{F}_d(p) \le 1, \forall d \in D \\ & \sum_{p\ni e}\sum_{d\in D} \mathcal{F}_d(p)\cdot d \le c(e), \forall e \in E \\ & \mathcal{F}_d(p) \ge 0, \forall d \in D, \forall p \in P_d \end{aligned} \tag{1}$$

Surrogate loss. The surrogate loss that approximates the (non-differentiable) total feasible flow is defined as the total flow intended to be routed (disregarding link capacities), penalized by total link overutilization. Using the above notations, the surrogate loss can be formally expressed as

$$\sum_{d\in D}\sum_{p\in P_d} \mathcal{F}_d(p)\cdot d - \sum_{e\in E}\max(0, \sum_{p\ni e}\sum_{d\in D} \mathcal{F}_d(p)\cdot d - c(e)).$$

B COMA* DETAILS

At a high level, COMA builds on the idea of counterfactual reasoning [62], deducing the answer to a "What if..." question: At the moment every agent is about to make a decision (*action*), what would be the difference in global reward if *only* one agent's action changes while the other agents' actions remain fixed? E.g., in the context of TE that aims to maximize the total flow, our COMA* reasons about: Compared with the current traffic allocations, how much would the total flow differ if we only reallocate the flows of one demand while keeping the allocations of the other demands unchanged? The performance difference measures the contribution of an agent's action to the overall reward. Specifically, the reward difference defines the "advantage" of the current joint action over the counterfactual baseline (where only one agent tweaks its action). The advantage is heavily used in this family of RL algorithms (known as actor-critics [31]) to effectively reduce the variance in training.

At each time step when a new traffic matrix arrives or any link capacity changes (e.g., due to a link failure), TEAL passes the flow embeddings (stored in PathNodes of FlowGNN) for the same demand to the RL agent i designated to manage the demand. We define these flow embeddings as the *state* s_i observed locally by agent i. Presented only with the local view captured by s_i, agent i makes an action a_i, a vector of split ratios that describes the allocation of the agent's managed demand. Let π_θ denote the policy network parameterized by θ shared by agents. Learning the weights θ with gradient descent is known as policy gradient [55], which typically requires a stochastic form $\pi_\theta(a_i|s_i)$ that represents the probability of outputting a_i given s_i. Since allocations are deterministic in TE, a common way that converts π_θ to stochastic is to have it output the mean and variance of a Gaussian distribution. During training, actions are sampled from the Gaussian distribution $a_i \sim \pi_\theta(\cdot|s_i)$, whereas the mean value of the Gaussian is directly used as the action during deployment.

We use $\mathbf{s}$ to denote the central state formed by all local states s_i, and $\mathbf{a}$ to denote the joint action formed by all local actions a_i. A reward $R(\mathbf{s}, \mathbf{a})$, such as the total flow, is available after all agents have made their decisions. To compute the advantage $A_i(\mathbf{s}, \mathbf{a})$ when *only* agent i alters its action, COMA proposes to estimate the expected return, namely a discounted sum of future rewards, obtained by taking the joint action $\mathbf{a}$ in central state $\mathbf{s}$. By comparison, our COMA* computes the expected return by leveraging the "one-step" nature of TE: an action (flow allocation) in TE does not impact the future states (traffic demands). Consequently, the expected return effectively equals the reward $R(\mathbf{s}, \mathbf{a})$ obtained at a single step. Moreover, suppose that agent i varies its action to a'_i while the other agents keep their current actions, the new joint action—denoted as $(\mathbf{a}_{-i}, a'_i)$—can be directly evaluated by simulating its effect, i.e., we compute the TE objective obtained if the new joint action were to be used. Putting everything together, COMA* computes the advantage for agent i as follows:

$$A_i(\mathbf{s}, \mathbf{a}) = R(\mathbf{s}, \mathbf{a}) - \sum_{a'_i} \pi_\theta(a'_i|s_i) R(\mathbf{s}, (\mathbf{a}_{-i}, a'_i)), \tag{2}$$

where we perform Monte Carlo sampling to estimate the counterfactual baseline, e.g., by drawing a number of random samples for $a'_i \sim \pi_\theta(\cdot|s_i)$. The gradient of θ is then given by

$$g = \mathbb{E}_\pi \left[\sum_i A_i(\mathbf{s}, \mathbf{a}) \nabla_\theta \log \pi_\theta(a_i|s_i) \right], \tag{3}$$

which is used for training the policy network with standard policy gradient. In practice, TEAL trains FlowGNN and the policy network of COMA* end to end, so θ represents all the parameters to learn in the end-to-end model, backpropagating gradients from the policy network to FlowGNN.

C ADMM DETAILS

In this section, we derive the ADMM iterates for the TE problem in Equation (1), reproduced here:

$$\begin{aligned} \text{maximize} \quad & \sum_{d\in D}\sum_{p\in P_d} \mathcal{F}_d(p)\cdot d \\ \text{subject to} \quad & \sum_{p\in P_d} \mathcal{F}_d(p) \le 1, \forall d \in D & (4) \\ & \sum_{p\ni e}\sum_{d\in D} \mathcal{F}_d(p)\cdot d \le c(e), \forall e \in E & (5) \\ & \mathcal{F}_d(p) \ge 0, \forall d \in D, p \in P_d. \end{aligned}$$

In order to apply ADMM which requires a specific form to optimize, we must decouple the constraints in the original problem. As Constraint (5) couples the edge traffic across paths and demands, we introduce dummy variables z_{pe} for each path p (from in any demand $d \in D$), and edge $e \in p$. We note that each path $p \in P_d$ uniquely stems from a particular demand d. Then, we replace Constraint (5) with the following constraints:

$$\sum_{p\ni e} z_{pe} \le c(e), \forall e \in E \tag{6}$$

$$\mathcal{F}_d(p)\cdot d - z_{pe} = 0, \forall d \in D, p \in P_d, e \in p. \tag{7}$$

Finally, we add slack variables $s = (s_{1d}, s_{3e})$, for all demands $d \in D$ and edges $e \in E$ respectively, to turn inequality in Constraint (4) and Constraint (6) into equality:

$$\begin{aligned}
\text{maximize} \quad & \sum_{d\in D}\sum_{p\in P_d} \mathcal{F}_d(p)\cdot d \\
\text{subject to} \quad & \sum_{p\in P_d} \mathcal{F}_d(p) + s_{1d} - 1 = 0, \forall d \in D && (4) \\
& \sum_{p\ni e} z_{pe} + s_{3e} - c(e) = 0, \forall e \in E && (6) \\
& \mathcal{F}_d(p)\cdot d - z_{pe} = 0, \forall d\in D, p\in P_d, e\in p && (7) \\
& \mathcal{F}_d(p) \geq 0, \forall d\in D, p\in P_d.
\end{aligned}$$

By introducing Lagrange multipliers $\lambda = (\lambda_1, \lambda_3, \lambda_4) \in \mathbb{R}^{|D|}\times\mathbb{R}^{|E|}\times\mathbb{R}^{|P||E|}$ and a penalty coefficient ρ, the augment Lagrangian for this transformed problem becomes

$$\mathcal{L}_\rho(\mathcal{F}, z, s, \lambda) = -\sum_{d\in D}\sum_{p\in P_d} \mathcal{F}_d(p)\cdot d + \lambda G(\mathcal{F}, z, s) + \frac{\rho}{2}\|G(\mathcal{F}, z, s)\|_2^2,$$

where $G(\mathcal{F}, z, s) = (G_1, G_3, G_4)^\top$ and

$$G_{1d} = \mathcal{F}_d(p) + s_{1d} - 1$$

$$G_{3e} = \sum_{p\ni e} z_{pe} + s_{3e} - c(e)$$

$$G_{4dpe} = \mathcal{F}_d(p)\cdot d - z_{pe}.$$

The ADMM iterates at step $k+1$ are then given by

$$\begin{aligned}
\mathcal{F}^{k+1} &:= \arg\min_{\mathcal{F}} \mathcal{L}_\rho(\mathcal{F}, z^k, s^k, \lambda^k) \\
z^{k+1} &:= \arg\min_{z} \mathcal{L}_\rho(\mathcal{F}^{k+1}, z, s^k, \lambda^k) \\
s^{k+1} &:= \arg\min_{s} \mathcal{L}_\rho(\mathcal{F}^{k+1}, z^{k+1}, s, \lambda^k) \\
\lambda^{k+1} &:= \lambda^k + \rho\cdot G(\mathcal{F}^{k+1}, z^{k+1}, s^{k+1})
\end{aligned}$$

with the initial iterates warm-started by the policy network.

D TOPOLOGY DETAILS

Table 3 provides additional details about the network topologies utilized in our study (SWAN is excluded from the table due to containing private information). In general, as the size of the network topology increases, the average shortest-path length and network diameter tend to become longer, with the exception of the ASN topology. This can be attributed to the presence of star-shaped clusters (ASes) within ASN. These clusters are interconnected, resulting in a strong connectivity at the cluster level.

	Average shortest-path length	Network diameter
B4	2.3	5
UsCarrier	12.1	35
Kdl	22.7	58
ASN	3.2	8

Table 3: Additional topology details.

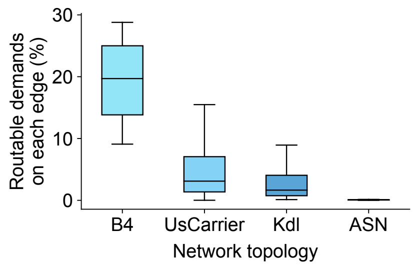

Figure 17: Percentage of routable demands for each edge, i.e., if (any of) the demand's preconfigured paths pass through the edge.

Meanwhile, we examine the percentage of demands (over the total number of demands) that are routable on each edge, i.e., if the edge lies on at least one of a demand's preconfigured paths, and plot the distributions in Figure 17. This figure reveals that as the network grows in size, each edge tends to serve a decreasing percentage of demands due to the sparser distribution of demands. Notably, the ASN topology exhibits an exceptionally low proportion of routable demands on each edge due to its distinctive characteristics.

E TE PERFORMANCE OVER TIME

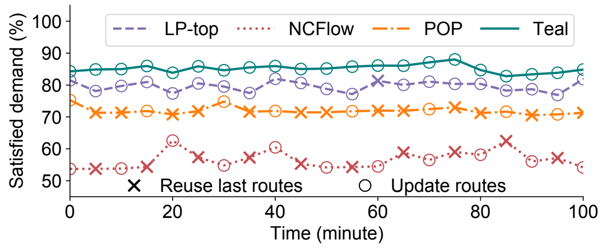

Figure 18: Allocation performance of schemes in response to changing demands over time on ASN. Teal consistently allocates the most demand in each time interval.

We present the allocation performance of different schemes in response to changing demands over time in Figure 18. With the run time fluctuating from a median of 200 s to the worst case of 450 s in Figure 7a, LP-top only uses updated routes at the end of the 5-minute interval and occasionally uses stale routes throughout the interval, leading to less demand satisfied. We also observe that NCFlow and POP can only compute a new allocation for every other or every third traffic matrix, and using stale routes from 5 or 10 minutes ago causes further performance degradation to the original suboptimal traffic allocation. In contrast, Teal consistently allocates the most demand in each time interval.